AIAA JOURNAL
Vol. 31, No. 3, March 1993

Rotational Compressible Inverse Design Method for Two-Dimensional, Internal Flow Configurations

V. Dedoussis,* P. Chaviaropoulos,† and K. D. Papailiou‡
National Technical University of Athens, 15710 Athens, Greece

The development of a rotational inviscid compressible inverse design method for two-dimensional internal flow configurations is described. Rotationality is due to incoming entropy gradient whereas total enthalpy is considered to be constant throughout the flowfield. The method is based on the potential function/stream function formulation. The Clebsch formulation is adopted to decompose the velocity vector into a potential and a rotational part. The physical space on which the boundaries of the flowfield are sought is mapped onto the (ϕ, ψ) space via a body-fitted coordinate transformation. A novel procedure based on differential geometry arguments is employed to derive the governing equation for the velocity. The velocity equation solved in conjunction with a transport equation for a thermal drift function provide the flowfield without any geometry feedback. An auxiliary orthogonal computational grid adapted to the solution is employed. Geometry is determined by integrating Frenet equations of the grid lines. Inverse calculation results are compared with results of direct "reproduction" calculations.

Nomenclature

a, b, c, d, e, f = velocity coefficients, Eq. (20)
c_p, c_v = specific heats
G_{mn} = metrics tensor of computational (ξ, η) coordinate system
g^m = contravariant base vector of natural (ϕ, ψ) coordinate system
g^{mn} = conjugate metrics tensor of natural (ϕ, ψ) coordinate system
g_{mn} = metrics tensor of natural (ϕ, ψ) coordinate system
h = enthalpy
$\boldsymbol{i}, \boldsymbol{j}, \boldsymbol{k}$ = unit base vectors of the (x, y, z) Cartesian coordinate system
$\boldsymbol{L}$ = position vector
M = Mach number
$[mn, l]$ = Christoffel symbol of first kind
p = static pressure
R = universal gas constant
R_{nmnm} = curvature of (n, m) surface
s = entropy
T = temperature
$\boldsymbol{V}$ = velocity vector
(x, y) = physical space Cartesian coordinate system
α = thermal drift function
β = angle between $\nabla\phi$, $\nabla\psi$
Γ^l_{mn} = Christoffel symbol of second kind
γ = specific heats ratio
δ^m_n = Kronecker delta
Θ_1 = angle between η = const lines and x axis
θ = angle between streamlines and x axis
κ_1 = signed curvature of η = const lines
(ξ, η) = orthogonal computational coordinate system
ρ = density
τ = drift function
(ϕ, ψ) = potential function, stream function natural coordinate system
Ω = vorticity vector

Subscripts
m, n, l, q = covariant tensor indices; 1, 2
o = known position indicator
ref = reference quantity
t = total quantity
ξ, η, ϕ, ψ = partial derivatives with respect to ξ, η, ϕ, or ψ, respectively

Superscripts
m, n, l, q = contravariant tensor indices; 1, 2

Received Nov. 14, 1991; revision received May 18, 1992; accepted for publication July 6, 1992.

*Research Engineer, Laboratory of Thermal Turbomachines, P.O. Box 64069. Member AIAA.
†Research Engineer, Laboratory of Thermal Turbomachines, P.O. Box 64069.
‡Professor, Mechanical Engineering, Laboratory of Thermal Turbomachines, P.O. Box 64069. Member AIAA.

Introduction

THE operation of propulsion systems and process industry equipment relies heavily on the nature of the flow in internal configurations such as air intakes, nozzles, ducts, etc. In designing such configurations, aerodynamicists aim to minimize or prevent losses associated with wall boundary-layer separation and/or the occurrence of a shock. It is known that the boundary-layer behavior, as well as the occurrence of a shock, is controlled by the characteristics of the pressure distribution along the walls of the channel. The need, therefore, of having accurate and efficient inverse design methods that provide the designer with the channel's geometry that corresponds to a prescribed wall pressure or velocity distribution is evident. A concise general review on aerodynamic shape design methods has been recently published by Dulikravich.[1]

In most of the cases inverse methods assume that the flow is both inviscid and irrotational. The purpose of this paper is to present an inverse two-dimensional compressible inviscid method *without* resorting to the rather restrictive assumption that the flow is irrotational. The present method assumes that the flow is isentropic along streamlines with total enthalpy being constant throughout the flowfield. Under those assumptions the rotational character of the flow, i.e., vorticity, is entirely due to the variation of entropy level between different streamlines. Thus the problem tackled by the method can be stated as follows:

Given a prescribed—target—velocity distribution along the solid boundaries and along the inlet and outlet of a channel, as well as prescribed entropy variation along the inlet, determine its geometry.

The method is based on the potential function/stream function formulation and in that respect is similar to the methods developed for irrotational flows by Stanitz.[2] The Clebsch formulation, also used by other authors,[3-5] is employed to decompose the velocity vector into a "potential" and a rotational part, the latter expressed as the product of a thermal drift function with the entropy gradient. Exploiting the fact that solid boundaries are streamlines, a body-fitted coordinate transformation is carried out that maps the physical (x, y) space (on which the geometry of the boundaries is sought) onto the potential function/stream function (ϕ, ψ) space. The potential function and the stream function are the independent nonorthogonal curvilinear coordinates.

An interesting novelty of the method is that the main second-order nonlinear elliptic partial differential equation (PDE) for the velocity magnitude is derived using differential geometry arguments rather than manipulating the basic flow equations themselves. Actually, one considers the metrics of the (ϕ, ψ) coordinates, which are expressed in terms of flow quantities, to be the metrics of the two-dimensional Euclidean space. In addition, one requires the curvature of the two-dimensional Euclidean space, being a flat one, to be zero. This equation, in conjunction with a transport equation for the thermal drift function of the Clebsch decomposition, provides the solution of the flowfield. The numerical integration of these equations is carried out on a (ξ, η) computational domain, with $\eta = \text{const}$ lines (parallel to) the streamlines and $\xi = \text{const}$ lines normal to them. This grid has to be introduced so that the resulting configuration has inlet and outlet sections normal to the streamlines.

The calculation procedure involves two main steps. In the first step the discretized governing equations are solved for the flow quantities using a fast iterative incomplete factorization scheme. Having calculated the flowfield, the geometry of the channel is determined, in a subsequent step, by straightforward integration of Frenet equations along potential lines and/or streamlines, or better along $\xi = \text{const}$ and/or $\eta = \text{const}$ lines.

Zannetti[6] proposed an inverse method for compressible inviscid rotational internal flows that solves the time-dependent Euler equations, the steady state providing the desired solution. The curvilinear grid employed to formulate the method is similar to the computational one used in the present method. It is formed by the streamlines of the steady solution and the lines orthogonal to them. Other time-dependent inverse techniques, which assume bodies with deformable walls,[7,8] as well as optimization design methods,[9] perform the calculation with time-consuming successive runs of direct Euler-type solvers in association with geometry feedbacks.

The method proposed in this paper, on the other hand, is fast and does not exhibit an iterative nature since the flowfield and geometry solutions are entirely independent. The reliability of the present method is quite clearly indicated by the satisfactory comparisons between direct "reproduction" and inverse calculations results presented in the paper.

Basic Assumptions and Equations

In the present inverse method it has been assumed that the flow is two dimensional, steady, compressible, inviscid, and adiabatic. The total enthalpy is assumed to be constant throughout the flowfield. On the other hand the flow is *not* considered to be homentropic. It is also assumed that the fluid is a perfect gas. It should be noted that the method has not been facilitated with any shock-capturing mechanism, and therefore it is limited to subsonic flow only.

In accordance with the aforementioned assumptions, the basic flow equations are

Continuity equation:

$$\nabla \cdot (\rho V) = 0 \tag{1}$$

Momentum equation:

$$T \nabla s + V \times \Omega = 0 \tag{2}$$

Energy equation:

$$V \cdot \nabla s = 0 \tag{3}$$

Gibbs equation:

$$T\, \mathrm{d}s = \mathrm{d}h - \mathrm{d}p/\rho \tag{4}$$

State equation for perfect gas:

$$p/\rho = R\, T \tag{5}$$

Equation (3) simply states that entropy is preserved along streamlines, i.e., that changes along streamlines are isentropic. It has been assumed, however, that the flow is *not* homentropic; therefore the entropy level of different streamlines may be different.

Equation (2) indicates that the rotational character of the flow is due to the entropy variation in the flowfield. Equivalently, this equation can be written as

$$\Omega = (V \times T \nabla s)/V^2 \tag{6}$$

Method Formulation

The formulation of the inverse method in terms of the potential function and the stream function is presented in this section. Details of the (ϕ, ψ) nonorthogonal curvilinear coordinate system are also included.

Clebsch Formulation

According to the Clebsch formulation, the velocity vector V is written as the sum of a "potential" and a rotational part in the following form[10]:

$$V = \nabla \phi + \alpha \nabla s \tag{7}$$

where ϕ is the "potential" function and α is a scalar coefficient representing a thermal drift function (its name will be justified later).

The term "potential" is included in quotation marks, since it indicates the irrotational character of the $\nabla\phi$ term rather than the existence of a potential function as such. From here onward quotation marks are dropped. The $\alpha \nabla s$ term accounts for the rotationality of the flow. Indeed, introducing Eq. (7) to the defining relation of Ω, it is seen that

$$\Omega = \nabla \alpha \times \nabla s \tag{8}$$

Transport Equation for Thermal Drift

Equation (8) is introduced into Eq. (2) to eliminate Ω. Carrying out the vector manipulations and noting that entropy is constant along streamlines, one gets the following transport equation for α:

$$V \cdot \nabla \alpha = T \tag{9}$$

Equation (9) indicates that the scalar quantity α is increasing monotonically along the streamlines in a way proportional to local temperature. This justifies the name "thermal drift" for the variable α. Alternatively, a drift function τ, defined as $(c_p \alpha + \frac{1}{2}\phi)/c_p T_t$, may be introduced, which is governed by the $V \cdot \nabla \tau = 1$ transport equation.

It should be noted that the present formulation is also capable of handling rotational flows with nonzero total enthalpy gradient, since in two-dimensional flows the total enthalpy and entropy gradients, being parallel, are related to one another via a scalar coefficient. It can be shown that this coefficient is constant along the streamlines. Its level on different streamlines is set from the specified entropy and total enthalpy distributions at the inlet section.

Stream Function

The stream function ψ is implicitly defined by the following relation:

$$\rho V = \nabla\psi \times k \tag{10}$$

where k is the unit vector normal to the plane of the flow. The stream function is defined in such a way so that the continuity equation (1) is satisfied identically.

Natural (ϕ, ψ) Curvilinear Coordinate System

The potential function and the stream function are considered to be the independent variables. Equations (7) and (10) provide the contravariant base of the (ϕ, ψ) coordinate system. Associating coordinate indices 1 and 2 with the ϕ and ψ coordinates, respectively, the contravariant base is

$$g^1 \equiv \nabla\phi = V - \alpha\nabla s \tag{11}$$

$$g^2 \equiv \nabla\psi = k \times \rho V \tag{12}$$

The dot product $\nabla\phi \cdot \nabla\psi$ is definitely nonzero since both ∇s and $\nabla\psi$ are normal to V [refer to Eqs. (3) and (10) respectively]. This indicates that $\phi = \text{const}$ and $\psi = \text{const}$ lines, i.e., potential lines and streamlines, are nonorthogonal. The difference from irrotational flows, where the (ϕ, ψ) coordinate system is orthogonal, is evident. The natural nonorthogonal (ϕ, ψ) curvilinear coordinate system used in the present method is shown schematically in Fig. 1.

Both the metrics and the conjugate (contravariant) metrics of the (ϕ, ψ) system, which actually define the body-fitted (x, y) to (ϕ, ψ) transformation, are evaluated using Eqs. (11), (12), and the following standard tensor relations[11]:

$$g^m \cdot g^n = g^{mn} \tag{13}$$

$$g^{ml} g_{ln} = \delta^m_n \tag{14}$$

with m, n, $l = 1, 2$; g_{ln} is the metrics tensor, and g^{ml} is the conjugate metrics tensor.

In terms of flow quantities, the metrics and the conjugate metrics of the (ϕ, ψ) coordinate system are

$$g_{11} = \frac{1}{V^2} \qquad g^{11} = \frac{V^2}{\sin^2\beta}$$

$$g_{22} = \frac{1}{(\rho V)^2 \sin^2\beta} \qquad g^{22} = (\rho V)^2 \tag{15}$$

$$g_{12} = g_{21} = \frac{-1}{\rho V^2 \tan\beta} \qquad g^{12} = g^{21} = \frac{\rho V^2}{\tan\beta}$$

where β is the angle between $\nabla\phi$ and $\nabla\psi$; see Fig. 1.

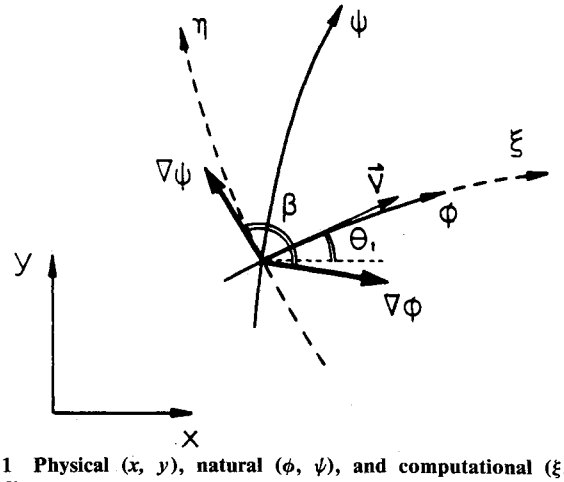

Fig. 1 Physical (x, y), natural (ϕ, ψ), and computational (ξ, η) coordinate systems.

Governing Equations

The objective of this section is to present and discuss the derivation of the equations that are actually solved by the present method for determining the flowfield.

Velocity Equation

The natural (ϕ, ψ) coordinate system has been set up on the physical two-dimensional (x, y) Euclidean space. The requirement that a space is Euclidean is that the curvature tensor of the space is zero, i.e., that the space is flat. In two-dimensional spaces the curvature tensor has one independent component,[11] R_{1212}, so the zero curvature condition reads

$$R_{1212} = 0 \tag{16}$$

where using generalized tensor notation[11]

$$R_{1212} = \frac{\partial}{\partial x^1}[22, 1] - \frac{\partial}{\partial x^2}[21, 1] + \Gamma^l_{21}[12, l] - \Gamma^l_{22}[11, l] \tag{17}$$

and

$$[mn, l] = \frac{1}{2}\left(\frac{\partial g_{ml}}{\partial x^n} + \frac{\partial g_{nl}}{\partial x^m} - \frac{\partial g_{mn}}{\partial x^l}\right) \tag{18}$$

$$\Gamma^q_{mn} = g^{ql}[mn, l] \tag{19}$$

with m, n, l, $q = 1, 2$. Equations (18) and (19) define the Christoffel symbols of the first and second kind, respectively.

Considering that the coordinate system describing the two-dimensional Euclidean space is the (ϕ, ψ) one and noting that its metrics are expressed as functions of flow quantities via Eqs. (15), condition (16) provides a PDE for the velocity magnitude V in terms of the density ρ and the local coordinate angle β. Associating coordinate indices 1 and 2 with the ϕ and ψ coordinates, respectively, one gets, after substitutions, the following equation:

$$a(\ell n V)_{\phi\phi} + b(\ell n V)_{\phi\psi} + c(\ell n V)_{\psi\psi} + d(\ell n V)_{\phi} + e(\ell n V)_{\psi} = f \tag{20}$$

where

$$a(\rho, \beta) = \frac{1}{\sin^2\beta}$$

$$b(\rho, \beta) = \frac{2\rho}{\tan\beta}$$

$$c(\rho, \beta) = \rho^2$$

$$d(\rho, \beta) = -\frac{1}{\sin^2\beta}\left[(\ell n\rho)_{\phi} + \rho\beta_{\psi} + \frac{2}{\tan\beta}\beta_{\phi}\right] \tag{21}$$

$$e(\rho, \beta) = \rho^2(\ell n\rho)_{\psi} - \frac{\partial}{\sin^2\beta}\beta_{\phi}$$

$$f(\rho, \beta) = -\frac{1}{\sin^2\beta}(\ell n\rho)_{\phi\phi} - \frac{\rho}{\tan\beta}(\ell n\rho)_{\phi\psi}$$

$$+\frac{(\ell n\rho)_{\phi}}{\sin^2\beta}\left[(\ell n\rho)_{\phi} + \rho\beta_{\psi} + \frac{3}{\tan\beta}\beta_{\phi}\right] - \frac{1}{\sin^2\beta\tan\beta}\beta_{\phi\phi}$$

$$-\frac{\rho}{\sin^2\beta}\beta_{\phi\psi} + \frac{2\rho}{\sin^2\beta\tan\beta}\beta_{\phi}\beta_{\psi} + \frac{2\cos^2\beta + 1}{\sin^4\beta}(\beta_{\phi})^2$$

and subscripts ϕ and ψ indicate corresponding partial derivatives.

The nonlinear elliptic second-order PDE, Eq. (20), is the main governing equation of the flowfield and represents the velocity equation sought. For irrotational flows, where $\beta = 90$ deg (potential lines are normal to streamlines), Eq. (20) is the same with that given by Stanitz.[12] It is emphasized that, in the

present method, the velocity PDE, Eq. (20), is derived in a novel way by considering differential geometry arguments only and *not* by manipulating the basic flow equations themselves (for comparison reasons the latter is described in detail in the Appendix). All of the necessary physical information is introduced to Eq. (20) in a natural, automatic way through the metrics relations of Eqs. (15). These define the transformation of the general and physically meaningless Cartesian (x, y) coordinate system to the physically meaningful (ϕ, ψ) system. Conclusively, Eq. (20) is derived by merely requiring the (ϕ, ψ) coordinate system to be meaningful with regard to both physics and geometry.

The coefficients of Eq. (20) are functions of ρ and β. To close the problem, one has to provide two equations for ρ and β.

Density Equation

The density is related to the velocity and entropy fields via the following standard equation:

$$\frac{\rho}{\rho_{\text{ref}}} = \left[\frac{1 + \frac{\gamma - 1}{2} M_{\text{ref}}^2 \left(1 - \frac{V^2}{V_{\text{ref}}^2}\right)}{e^{(s - s_{\text{ref}})/c_v}} \right]^{1/(\gamma - 1)} \tag{22}$$

where γ is the ratio of specific heats c_p/c_v.

In the present method the relative entropy level, $(s - s_{\text{ref}})$, is set a priori. The Mach number at the reference point, M_{ref}, indicating the degree of compressibility of the fluid or implicitly setting the level of total enthalpy in the flow, is also set a priori.

Coordinate Angle Equation

Definition (7) indicates that the thermal drift α is related in some way to the angle β formed between $\nabla\phi$ and $\nabla\psi$, appearing in the velocity equation (20). The relation between α and β can be inferred by considering the mixed conjugate metrics element g^{12}. From its definition g^{12} can be written as [see Eq. (11) and Fig. 1]

$$g^{12} \equiv \boldsymbol{g}^1 \cdot \boldsymbol{g}^2 = (\boldsymbol{V} - \alpha \nabla s) \cdot \nabla\psi = |\nabla\phi| \; |\nabla\psi| \cos\beta \tag{23}$$

which, after manipulations, gives

$$\tan\beta = -1/(\alpha s_\psi \rho) \tag{24}$$

The thermal drift equation (9) and Eqs. (22) and (24) (supplemented by a temperature equation), in conjunction with the velocity equation (20), form a closed set of equations. This set of equations is used by the present method for the calculation of the flowfield.

As Eq. (22) indicates, it is more convenient to carry out the calculation in terms of dimensionless quantities. Reference quantities representing the corresponding ones at an arbitrarily chosen point in the field, referred to as the reference point (the point where $V/V_{\text{ref}} = 1$), are chosen for the basic dependent variables V, ρ, and T. The relative entropy level is made dimensionless with specific heat c_v. A reference length is also introduced.

(ξ, η) Computational Domain of Integration

Having expressed the governing equations using ϕ and ψ as independent variables, the obvious integration domain in the (ϕ, ψ) plane appears to be the rectangular one, with ϕ = const lines corresponding to the inlet and outlet sections of the channel and ψ = const lines corresponding to its lower and upper solid boundaries. In rotational flows, potential, ϕ = const lines and streamlines, ψ = const, lines are nonorthogonal, indicating that the inlet and outlet sections, calculated as potential lines, would *not* be normal to the flow direction.

In general it is desirable that the computed channel has inlet and outlet sections normal to the streamlines. To achieve this, one has to integrate the governing equations in an irregular domain, in the (ϕ, ψ) plane, say a trapezoid, whose parallel sides are ψ = const lines and correspond to the channel's solid walls.

An auxiliary numerical transformation[13] is employed that maps the required irregular (ϕ, ψ) integration domain to a rectangular domain in a computational (ξ, η) plane, with square unit computational cells. The η = const lines correspond to the uniformly distributed ψ = const lines, streamlines, i.e., $\psi_\xi = 0$. The ξ = const family lines, whose limiting values correspond to the inlet and outlet sections, are defined in the (ϕ, ψ) plane according to the relation

$$\phi_\eta = -\alpha s_\eta \tag{25}$$

Equation (25) is derived by requiring the dot product $\boldsymbol{V} \cdot d\boldsymbol{L}$, $d\boldsymbol{L}$ being the infinitesimal vector tangential to ξ = const lines, to be zero. Namely, one requires ξ = const lines to be normal to the streamlines, η = const lines. Thus, *the resulting* (ξ, η) *body-fitted coordinate system is orthogonal.*

Equation (25), which actually defines the (ξ, η) grid, indicates that this grid depends on the flow solution itself, simply because α is a prime variable being calculated in the procedure (note that s_η is set up a priori). The (ξ, η) grid is continuously reconstructed (adapted) to the currently available field (thermal drift distribution) within the iterative flowfield calculation procedure. It is evident, therefore, that the present inverse method could be categorized as an adaptive grid technique.

Flowfield Calculation

Numerical Method

The transformed governing equations (20), (9), and (22), which are integrated in the (ξ, η) plane, form a set of nonlinear equations. Some sort of iterative solution procedure is therefore required.

The velocity equation, which itself is a nonlinear elliptic PDE (in subsonic flows only), is linearized by assuming that the distributions of ρ and β are known. Discretizing partial derivatives employing central second-order accurate differencing, a system of algebraic equations with a nine-diagonal banded nonsymmetric characteristic matrix is obtained. This is solved using the modified strongly implicit procedure,[14] which is an incomplete lower-upper approximate factorization procedure.

Once the velocity field is determined, the transport equation for the thermal drift is integrated along streamlines using a second-order accurate Runge-Kutta scheme. The newly calculated α distribution provides a better estimate for β, via Eq. (24). This distribution, in conjunction with a better estimate for ρ calculated from Eq. (22), is used to update the assumed ρ and β distributions in the velocity equation.

Iterations continue until velocity convergence is achieved. Convergence is established within 10^{-7} tolerance for the rms value of the velocity equation residual. Computational experiments showed that under-relaxing the velocity solution with a relaxation factor of the order of 0.4–0.5 was necessary to both achieve and accelerate convergence.

The procedure just described provides the solution of the flowfield in a self-contained and independent manner without requiring any feedback from the geometry. This characteristic renders the present method a fast one.

It should be added that the central differencing practice for the velocity equation limits the present method to subsonic flows only, where the character of the equation is elliptic. When, however, a considerable part of the flowfield is supersonic, this practice leads to erroneous results (if, of course, convergence is achieved). In such a case upwind differencing and/or artificial viscosity are required.

Boundary Conditions

The velocity equation (20), being a second-order elliptic PDE requires boundary conditions all around the integration

domain. The velocity magnitude is specified (Dirichlet-type condition) on the solid walls—target velocity distribution—as $V = V(\phi)$ and in the inlet and outlet sections as $V = V(\psi)$. Taking into account the one-to-one correspondence of the (ϕ, ψ) to (ξ, η) transformation, boundary velocity distributions could be considered as $V = V(\xi)$ and $V = V(\eta)$ in the (ξ, η) plane of integration.

The potential ϕ is related to the arc length L on the solid wall via the relation $d\phi = V \cdot dL$. It is obvious, therefore, that $V = V(\phi)$ could be considered to represent a $V = V(L)$ distribution. The designer usually specifies the latter rather than the former.

The thermal drift equation (9) is a first-order transport equation requiring Dirichlet-type boundary conditions along the inlet section only. In the present method, α is specified as an arbitrary constant along the inlet section. As is indicated by Eq. (24), α controls the size of $\tan \beta$. It is a measure, therefore, of the local skewness of the (ϕ, ψ) coordinate system employed, implicitly defining the position of potential lines with respect to streamlines. The arbitrary character of the boundary condition was also verified computationally, where results for different values of α were identical. Generally speaking, less skewed (ϕ, ψ) systems provide a better description of the flow. Referring to Eq. (24), it is clear that the degree of skewness is proportional to the size of α. It is desirable, therefore, to keep the size of α as low as possible. In view of the fact that α increases monotonically along the streamlines, negative values for α are specified in the inlet section.

Geometry Determination

The geometry of the channel is determined by integrating Frenet equations of $\eta = \text{const}$ and/or $\xi = \text{const}$ lines in the physical (x, y) plane. In the case of two-dimensional lines, the integration of Frenet equations, say of $\eta = \text{const}$ lines shown in Fig. 1, is simplified, providing the following relations for their Cartesian coordinates:

$$x_1 = x_{1o} + \int_{\xi_o}^{\xi} \cos \Theta_1 \sqrt{G_{11}}\, d\xi \tag{26}$$

$$y_1 = y_{1o} + \int_{\xi_o}^{\xi} \sin \Theta_1 \sqrt{G_{11}}\, d\xi \tag{27}$$

where Θ_1 is the angle between $\eta = \text{const}$ line, and the x axis is given by

$$\Theta_1 = \Theta_{1o} + \int_{\xi_o}^{\xi} \kappa_1 \sqrt{G_{11}}\, d\xi \tag{28}$$

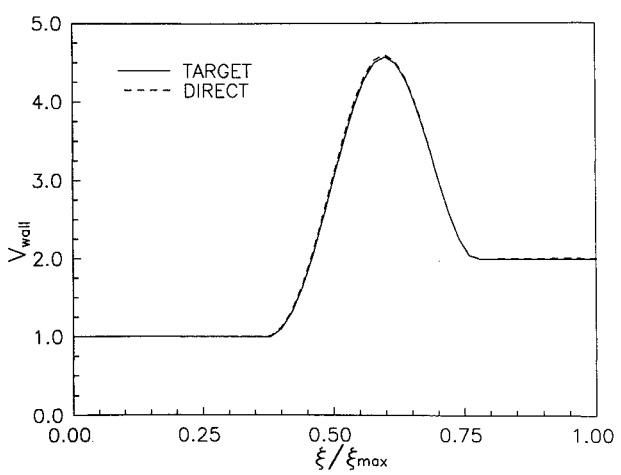

Fig. 2 Target and direct calculation wall velocity distribution for rotational nozzle case.

Relations analogous to Eqs. (26–28) hold for the $\xi = \text{const}$ lines.

In relation (28), κ_1 is the signed curvature of $\eta = \text{const}$ lines. For the orthogonal (ξ, η) coordinate system, κ_1 is

$$\kappa_1 = \Gamma^2_{11} \sqrt{G_{22}}/G_{11} \tag{29}$$

where the Christoffel symbol and the metrics with capital letters refer to the (ξ, η) coordinate system. The latter are related to those of the (ϕ, ψ) system, given by relations (15), through the following generalized tensor transformation[11]:

$$G_{mn} = \frac{\partial x^q}{\partial \bar{x}^m} \frac{\partial x^l}{\partial \bar{x}^n} g_{ql} \tag{30}$$

with $m, n, l, q = 1, 2$. Coordinates x^1 and x^2 are associated with ϕ and ψ, and $\bar{x}^1$ and $\bar{x}^2$ with ξ and η, respectively.

The drawback of the numerical integrations, Eqs. (26–28), is that the error is accumulating as the integration proceeds. Stanitz[12] argues that inaccuracies associated with this error accumulation are minimized if one determines the central streamline of the channel, $\eta = \text{const}$ line, first and then, starting from it, determines the upper and lower walls by integrating along $\xi = \text{const}$ lines. This practice has been adopted in this work. Constants of integrations in Eqs. (26–28) for the central streamline have been arbitrarily set to zero.

Computational Results and Discussion

The inverse design method proposed here has been applied to determine the geometry of a symmetric convergent-divergent nozzle and that of an elbow channel, with irrotational and rotational flow. To establish the reliability of the design method, inverse calculation results are compared with those of direct "reproduction" calculations. The term "reproduction" is used in the sense that the flowfield solution of a direct method applied to the geometry (and using the grid produced by the inverse method) should ideally be the same as, indeed should *reproduce*, the flow solution of the inverse method.

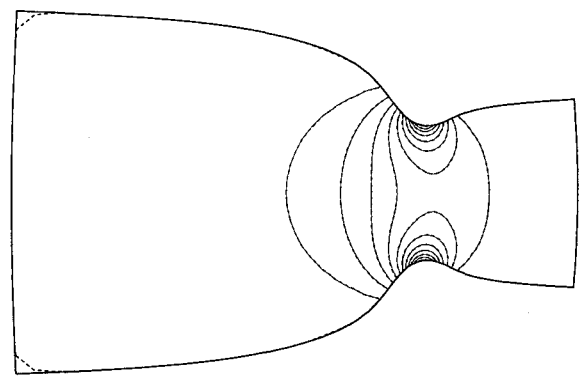

Fig. 3 Mach contours of inverse (——) and direct (----) methods for irrotational nozzle case ($M_{min} = 0.15$, $\Delta M = 0.05$).

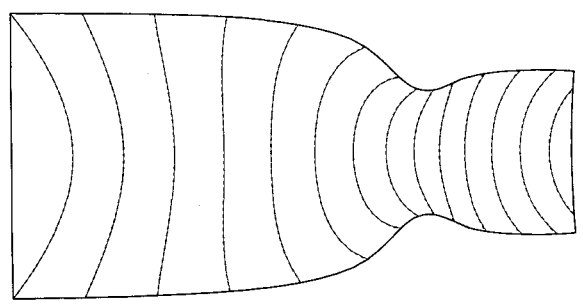

Fig. 4 Potential lines of inverse (——) and direct (----) methods for rotational nozzle case ($\phi_{min} = 0$, $\Delta\phi = 4$).

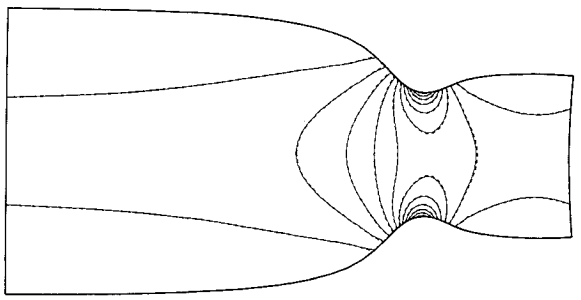

Fig. 5 Mach contours of inverse (——) and direct (----) methods for rotational nozzle case ($M_{min} = 0.15$, $\Delta M = 0.05$).

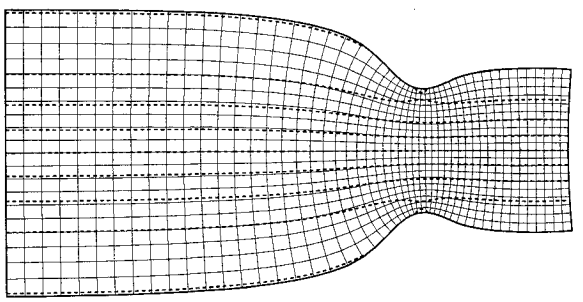

Fig. 6 Grid and vorticity contours for rotational nozzle case ($\Omega_{min} = -0.08$, $\Delta\Omega = 0.02$).

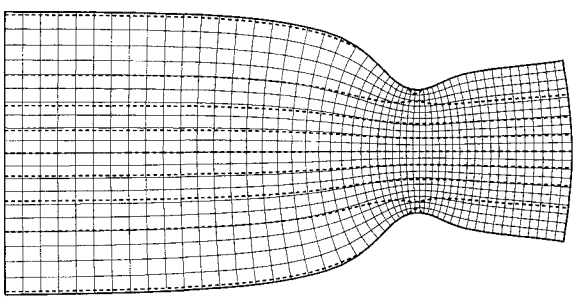

Fig. 7 Grid and vorticity contours for rotational nozzle case with uniform outlet velocity ($\Omega_{min} = -0.08$, $\Delta\Omega = 0.02$).

The direct method used for the comparisons employs the Clebsch formulation discussed in the previous sections and carries out the calculation in terms of ϕ, α, and s.

In all of the rotational test cases, the entropy distribution is set a priori not in an entirely arbitrary manner. Entropy level of different streamlines at the inlet section is computed according to the relation

$$s_\eta = -(V/T)V_\eta \tag{31}$$

This relation is derived by assuming that the vorticity that corresponds to the velocity gradient at the inlet is compatible with the one that corresponds to the entropy gradient. In addition, it is necessary to assume that the inlet section is straight and that the flow is evolving very slowly in the vicinity of the inlet, i.e., that streamlines there are almost parallel. A posteriori observations of the rotational cases results satisfy these conditions to a great extent. Actually, it can be shown that specifying both the velocity and entropy gradients along the inlet section is equivalent to specifying the streamwise gradient of the velocity. The solution (geometry), therefore, near the inlet adjusts itself, so that the streamwise velocity gradient is the same as the implicitly imposed one.

Results for the symmetric convergent-divergent nozzle are presented in Figs. 2–7. Calculations were carried out with a 51×21 grid with $\Delta\psi = 1$, $\Delta\phi_{lower\ wall} = 1$, and $M_{ref} = 0.15$. Imposed—target—wall velocity distribution for both the irrotational and rotational cases is shown in Fig. 2. The nonconstant part of this distribution is described by a sinusoidal function with linearly increasing amplitude. For the irrotational case, uniform inlet and outlet velocity distributions are specified. In the rotational case, symmetric parabolic velocity profiles with peak values 1.4 and 2.5 in the inlet and outlet sections, respectively, are assumed.

Wall velocity distribution for the rotational case calculated with the direct method is also included in Fig. 2. This distribution agrees very well with the target distribution. Small discrepancies observed in the divergent part of the nozzle may very well be due to the fact that the integration of the thermal drift transport equation (9) in the direct method is carried out with a first-order accurate scheme. Calculated flowfield distributions of the Mach number, which achieves values as high as 0.72, and the potential function are shown in Figs. 3–5. Inverse and direct method results, denoted by solid and dashed lines, respectively, are entirely symmetric. Their agreement is very good, indicating the reliability of the present method.

Comparing the shapes of the irrotational and rotational nozzle, one observes that the latter is narrower than the former. This is expected simply because in the rotational case the inlet velocity is higher, so that the fixed mass passing through it, indicated by the difference of the limiting stream function values, requires a smaller inlet width.

The (ξ, η) grid *generated* by the inverse method for the rotational case is shown in Fig. 6. This is indeed orthogonal in accordance with Eq. (25). Figure 7 presents the inverse solution for the rotational case with uniform outlet velocity distribution. Changes are noticeable in the divergent part of the

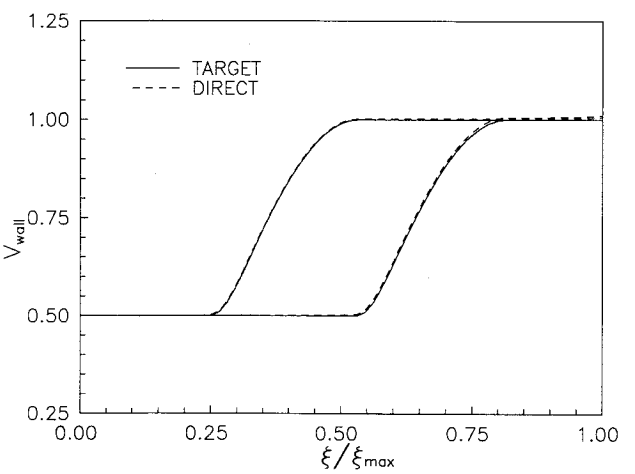

Fig. 8 Target and direct calculation wall velocity distributions for rotational elbow channel case.

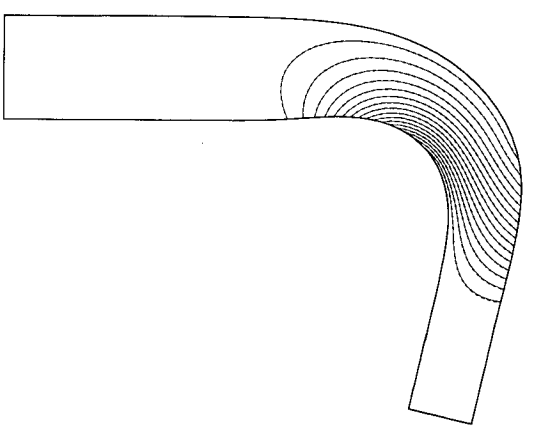

Fig. 9 Mach contours of inverse (——) and direct (----) methods for irrotational elbow channel case ($M_{min} = 0.4$, $\Delta M = 0.025$).

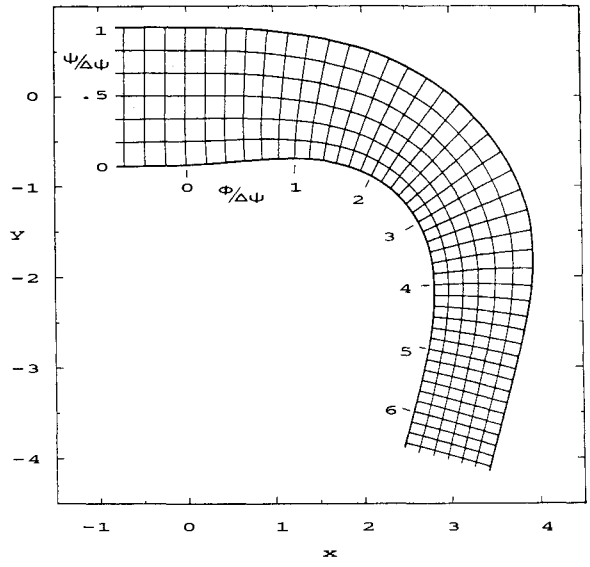

Fig. 10 Stanitz[12] results for irrotational elbow channel case (exit Mach no. = 0.7993).

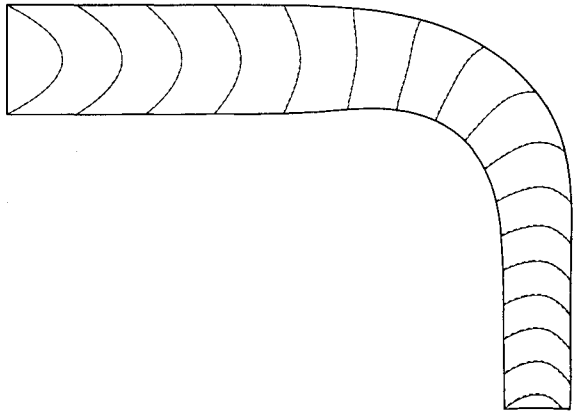

Fig. 11 Potential lines of inverse (——) and direct (----) methods for rotational elbow channel case ($\phi_{min} = 0$, $\Delta\phi = 4$).

nozzle only, mainly resulting in an opening of the angle of the nozzle. Dashed lines in Figs. 6 and 7 are calculated vorticity contours. These are almost identical to streamlines, a fact that is nearly true for two-dimensional compressible flows.

For the elbow channel case, calculations were performed with a 65×17 grid with $\Delta\psi = 0.5$, $\Delta\phi_{lower\ wall} = 1$. Target wall velocity distributions on the upper and lower channel walls for both the irrotational and rotational cases are shown in Fig. 8. Their characteristic is that the flow on both walls of the channel never decelerates.

In the irrotational case, uniform velocity distributions are imposed at the inlet and outlet sections, the Mach number at the outlet being $M_{ref} = 0.7993$. This test case corresponds to the well-documented elbow case of Stanitz.[12] The Mach number contours calculated with the inverse and direct methods, presented in Fig. 9, are almost identical. The geometry of the channel agrees very well with that calculated by Stanitz,[12] as shown in Fig. 10.

In the rotational elbow case, symmetric parabolic velocity profiles with peak values of 0.58 and 1.1 are imposed with $M_{ref} = 0.6$. Wall velocity distributions calculated with the direct method are compared with the target ones in Fig. 8. They exhibit very satisfactory agreement. Results for the potential function, the Mach number, and the thermal drift function are presented in Figs. 11–13, respectively. Inverse method results

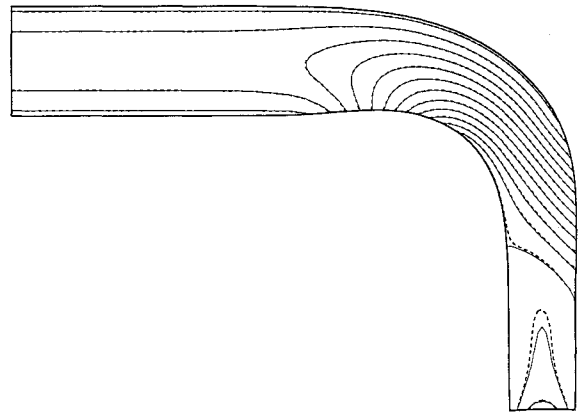

Fig. 12 Mach contours of inverse (——) and direct (----) methods for rotational elbow channel case ($M_{min} = 0.3$, $\Delta M = 0.025$).

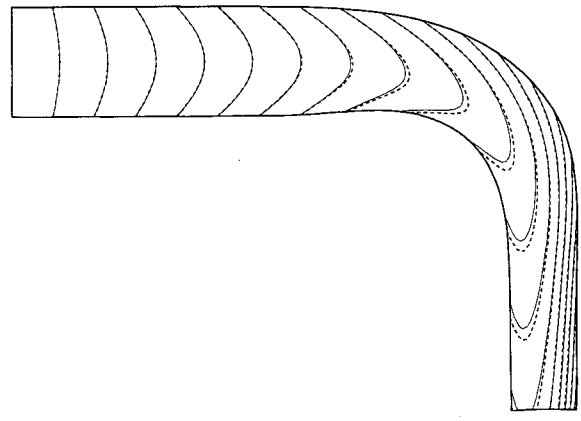

Fig. 13 Thermal drift function contours of inverse (——) and direct (----) methods for rotational elbow channel case ($\alpha_{min} = -80$, $\Delta\alpha = 10$).

agree quite well with those of the direct method (compare solid and dashed line contours, respectively). Small discrepancies observed near the outlet of the channel are possibly due to inaccuracies involved with the integration of the thermal drift equation in the direct method.

Conclusions

The development of an inverse method applicable to the design of internal configurations with rotational compressible flow has been described. The method assumes that the flow is inviscid, adiabatic, and subsonic with constant total enthalpy. It is also assumed that the entropy level of different streamlines is different, imposing the rotational character.

The method developed is based on the potential function/stream function formulation. The Clebsch formulation has been adopted to decompose the velocity vector into a potential and a rotational part, which is related to the entropy gradient via a thermal drift function, governed by a transport equation.

A novel procedure is proposed for deriving the velocity equation, employing differential geometry principles only. Considering ϕ and ψ as the independent variables, the metrics of the two-dimensional Euclidean space are expressed in terms of flow quantities. The requirement that the Euclidean space is flat and has zero curvature provides an elliptic equation for the velocity magnitude.

The set of the velocity and the thermal drift equations, in conjunction with a density equation, are solved for the flowfield on an auxiliary orthogonal computational grid automatically produced by the solution itself. The method is fast because it does not rely on any feedback from the geometry. The latter is determined independently by straightforward integration of Frenet equations along the grid lines.

Calculated results are presented for a symmetric convergent-divergent nozzle and an elbow channel. Both sets of results exhibit remarkable agreement with the results of a direct solution technique when applied to the geometry that had been determined by the inverse method (actually they were reproduced). These favorable comparisons indicate the reliability of the inverse method proposed.

Appendix

The purpose of the Appendix is to derive the velocity equation (20) using the basic flow equations.

Eliminating the temperature from Eq. (6), using Eq. (9), we get

$$\Omega \equiv \nabla \times V = (V \cdot \nabla \alpha)\ (V \times \nabla s)/V^2 \tag{A1}$$

Taking into account the energy equation (3) and noting that $V = V(\cos\theta \boldsymbol{i} + \sin\theta \boldsymbol{j})$, where θ is the angle between V and the x axis, Eq. (A1) is written in the (ϕ, ψ) coordinate system as

$$V^2\left[-\frac{1}{\tan\beta}(\ell n V)_\phi - \rho(\ell n V)_\psi + \theta_\phi\right]\boldsymbol{k} = \rho V^2(\alpha s_\psi)_\phi\, \boldsymbol{k} \tag{A2}$$

Introducing Eq. (24) into Eq. (A2) and rearranging, we get

$$\frac{1}{\tan\beta}(\ell n V)_\phi + \rho(\ell n V)_\psi - \rho\left(\frac{1}{\rho\tan\beta}\right)_\phi = \theta_\phi \tag{A3}$$

The continuity equation (1) expressed in the (ϕ, ψ) coordinate system is

$$\frac{1}{\rho}(\ell n V)_\phi + \frac{1}{\rho}(\ell n \rho)_\phi + \frac{\theta_\phi}{\rho\tan\beta} = -\theta_\psi \tag{A4}$$

Equation (A3) is used to eliminate θ_ϕ from Eq. (A4), resulting in

$$\frac{1}{\rho\sin^2\beta}(\ell n V)_\phi + \frac{1}{\tan\beta}(\ell n V)_\psi + \frac{1}{\rho}(\ell n \rho)_\phi - \frac{1}{\tan\beta}\left(\frac{1}{\rho\tan\beta}\right)_\phi = -\theta_\psi \tag{A5}$$

The velocity equation (20) is obtained by differentiating Eqs. (A3) and (A5) with respect to ψ and ϕ, respectively, and eliminating $\theta_{\phi\psi}$. In fact, the elimination of $\theta_{\phi\psi}$ requires that $\theta_{\phi\psi} = \theta_{\psi\phi}$. It can be shown that this is equivalent to the requirement that the R_{1212} curvature (or the Gaussian curvature) is zero, which is used in the present work.

Acknowledgment

Part of this work was financed by the DG XII of the European Economic Community in the context of the BRITE EURAM AERO-0026-C(TT) "Optimum Design in Aerodynamics" Project.

References

[1]Dulikravich, G. S., "Aerodynamic Shape Design," Special Course on Inverse Methods for Airfoil Design for Aeronautical and Turbomachinery Applications, AGARD Rept. 780, May 1990.

[2]Stanitz, J. D., "A Review of Certain Inverse Methods for the Design of Ducts with 2- or 3-Dimensional Flow," *Applied Mechanics Review*, Vol. 41, No. 6, 1988, pp. 217–238.

[3]Ecer, A., and Akay, H. U., "A Finite Element Formulation for Steady Transonic Euler Equations," *AIAA Journal*, Vol. 21, No. 3, 1983, pp. 343–350.

[4]Hawthorne, W. R., Wang, C., Tan, C. S., and McCune, J. E., "Theory of Blade Design for Large Deflections: Part I—Two-Dimensional Cascade," *American Society of Mechanical Engineers Journal of Engineering for Gas Turbines and Power*, Vol. 106, No. 2, 1984, pp. 346–353.

[5]Hawthorne, W. R., and Tan, C. S., "Design of Turbomachinery Blading in Three-Dimensional Flow by the Circulation Method: A Progress Report," *Proceedings of the 2nd International Conference on Inverse Design Concepts and Optimization in Engineering Sciences, ICIDES-II* (University Park, PA), edited by G. S. Dulikravitch, Oct. 1987, pp. 207–226.

[6]Zannetti, L., "A Natural Formulation for the Solution of 2-D or Axisymmetric Inverse Problems," *International Journal for Numerical Methods in Engineering*, Vol. 22, No. 2, 1986, pp. 451–463.

[7]Zannetti, L., "Time Dependent Method to Solve Inverse Problems for Internal Flows," *AIAA Journal*, Vol 18, No. 7, 1980, pp. 754–758.

[8]Zannetti, L., and Pandolfi, M., "Inverse Design Technique for Cascades," NASA CR-3836, 1984.

[9]Van den Dam, R. F., Boerstoel, J. W., and Daniels, H. A. M., "Optimization in Design Processes: An Informatics Point of View," *Proceedings of the International Conference on Inverse Design Concepts and Optimization in Engineering Sciences, ICIDES-I* (Austin, TX), edited by G. S. Dulikravitch, Oct. 1984, pp. 145–174.

[10]Lamb, H., *Hydrodynamics*, 6th ed., Dover, New York, 1945, p. 248.

[11]Aris, R., *Vectors, Tensors, and the Basic Equations of Fluid Mechanics*, Prentice-Hall, Englewood Cliffs, NJ, 1962, Chap. 7.

[12]Stanitz, J. D., "Design of Two-Dimensional Channels with Prescribed Velocity Distributions Along the Channel Walls," NACA Rept. 1115, 1953.

[13]Thompson, J. F., "Numerical Solution of Flow Problems Using Body-Fitted Coordinate Systems," *Computational Fluid Dynamics*, edited by W. Kollmann, Hemisphere, New York, 1980, pp. 1–98.

[14]Zedan, M., and Schneider, G. E., "A Three-Dimensional Modified Strongly Implicit Procedure for Heat Conduction," *AIAA Journal*, Vol. 21, No. 2, 1983, pp. 295–303.